Four-Coordinate Dimethylgallium Compounds Vary in Stability toward Hydrolysis

Robert W. Chesnut,[‡] Richard R. Cesati III,[†] Cathy S. Cutler,[§] Sara L. Pluth,[†] and John A. Katzenellenbogen*,[†]

Department of Chemistry, University of Illinois, Urbana, Illinois 61801, Department of Chemistry, Eastern Illinois University, Charleston, Illinois 61920, and Division of Radiological Sciences, Mallinckrodt Institute of Radiology, Washington University Medical School, St. Louis, Missouri 63110

Four-coordinate dimethylgallium complexes were prepared by the reaction of dimethylgallium hydroxide with bidentate Lewis bases and evaluated for their stability toward decomplexation in water, a key property in determining their potential usefulness as radiopharmaceuticals, particularly those targeted at specific receptor proteins. Model compounds from six structural classes, containing bidentate ligands with oxygen−oxygen, oxygen−nitrogen, and sulfur−nitrogen donor atoms, were prepared from the ligand and dimethylgallium hydroxide; they were characterized spectroscopically and, in two cases, by X-ray crystallography. The percentage decomplexation of the stable $(CH_3)_2Ga^+$ unit from the Lewis base when exposed to 1000 equiv of water in acetone-d_6, determined by ^1H NMR, was used as a measure of the relative hydrolytic stability of each compound. Among the compounds we have investigated, the percent hydrolysis under these conditions ranged from 10% to 100%, the most hydrolytically stable compounds proving to be those based on an *N*-alkylsalicylaldimidate donor.

Introduction

Radioisotopes of gallium, as the trication Ga^{3+}, are regularly used for medical imaging, and other gallium compounds are being investigated for their potential as radiopharmaceuticals.[1−3] These radiodiagnostic agents consist of ligands chelated to either ^{67}Ga, ^{68}Ga, or ^{66}Ga radioisotopes.[4−6] Since the ^{66}Ga and ^{68}Ga isotopes are positron-emitting nuclides with convenient half-lifes, we became interested in incorporating gallium into estrogens for imaging of breast tumors by PET.

Breast tumors can be imaged by the binding of appropriately labeled estrogens to the estrogen receptor (ER), which is found in many tumors, and these images provide useful prognostic information concerning cancer stage and tumor responsiveness to hormone therapy.[7−13]

So far, however, breast tumor imaging through the ER has been accomplished only with a number of radio-halogen-labeled estrogens. The availability of the halogen radionuclides needed to produce these ER-binding agents, however, is limited, either by their short half-lives (e.g., for ^{18}F, $t_{1/2}$ = 110 min) or by difficulties in their production (e.g., production of ^{123}I requires high-energy cyclotrons). Because ^{66}Ga and ^{67}Ga have relatively long half-lives ($t_{1/2}$ = 9.4 h and 3.3 days, respectively) and ^{68}Ga ($t_{1/2}$ = 68 min) is available from a long-lived ^{68}Ge ($t_{1/2}$ = 288 days) generator, replacing the radiohalogen in these imaging agents with these gallium radionuclides would make them more widely available and might also simplify their preparation.

When gallium is used as the citrate salt of the Ga^{3+} cation, most in vivo transport and uptake of this cation is mediated by iron-binding proteins, principally transferrin, because of the similar ionic radii of Ga^{3+} and Fe^{3+}.[14] If undesirable for a given procedure, binding of Ga^{3+} to transferrin can be prevented by the use of high-affinity multidentate ligands, generally hexadentate ones.[15] An alternative form of gallium that has been evaluated for radiopharmaceutical purposes is $(CH_3)_2$-

* Address correspondence to: John A. Katzenellenbogen, Department of Chemistry, University of Illinois, 461 Roger Adams Laboratory, Box 37-5, 600 S. Mathews Ave., Urbana, IL 61801. Telephone: (217) 333-6310. Fax: (217) 333-7325. E-mail: jkatzene@uiuc.edu.

† University of Illinois.
‡ Eastern Illinois University.
§ Mallinckrodt Institute of Radiology.

(1) Green, M. A.; Welch, M. J. *Nucl. Med. Biol.* **1989**, *16*, 435.
(2) Green, M. A. *New Trends in Radiopharmaceutical Synthesis, Quality Assurance, and Regulatory Control*; Plenum Press: New York, 1991.
(3) Green, M. A. *Adv. Met. Med.* **1993**, *1*, 75.
(4) Graham, M. C.; Pentlow, K. S. *Med. Phys.* **1997**, *24*, 317.
(5) Szelecsényi, F.; Boothe, T. E.; Tavano, E.; Plitnikas, M. E.; Tárkány, F. *Appl. Radiat. Isot.* **1994**, *45*, 473.
(6) Goethals, P.; Coene, M.; Slegers, G.; Vogelaers, D.; Everaert, J.; Lemahieu, I.; Colardyn, F.; Heyndrickx, G. R. *Eur. J. Nucl. Med.* **1990**, *16*, 237.
(7) Rijks, L. J. M.; Bakker, P. J. M.; Vantienhoven, G.; Noorduyn, L. A.; Boer, G. J.; Rietbroek, R. C.; Taat, C. W.; Janssen, A. G. M.; Veenhof, C. H. N.; Vanroyen, E. A. *J. Clin. Oncol.* **1997**, *15*, 2536.
(8) Rijks, L. J. M.; Sokole, E. B.; Stabin, M. G.; de Bruin, K.; Janssen, A. G. M.; van Royen, E. A. *Eur. J. Nucl. Med.* **1998**, *25*, 40.

(9) Mintun, M. A.; Welch, M. J.; Siegel, B. A.; Mathias, C. J.; Brodack, J. W.; McGuire, A. H.; Katzenellenbogen, J. A. *Radiology* **1988**, *169*, 45.
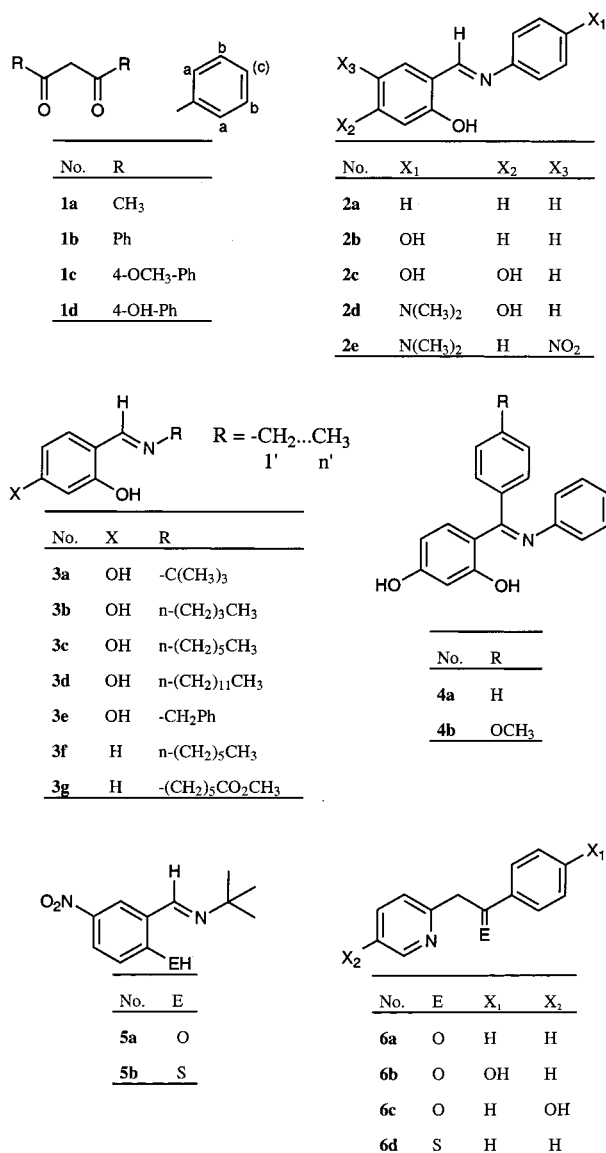(10) McGuire, A. H.; Dehdashti, F.; Siegel, B. A.; Lyss, A. P.; Brodack, J. W.; Mathias, C. J.; Mintun, M. A.; Katzenellenbogen, J. A. *J. Nucl. Med.* **1991**, *32*, 1526.
(11) Cummins, C. H. *Steroids* **1993**, *58*, 245.
(12) Pavlik, E. J.; Nelson, K.; Gallion, H. H.; van Nagell, J. R., Jr.; Donaldson, E. S.; Shih, W. J.; Spicer, J. A.; Preston, D. F.; Baranczuk, R. J.; Kenady, D. E. *Cancer Res.* **1990**, *50*, 7799.
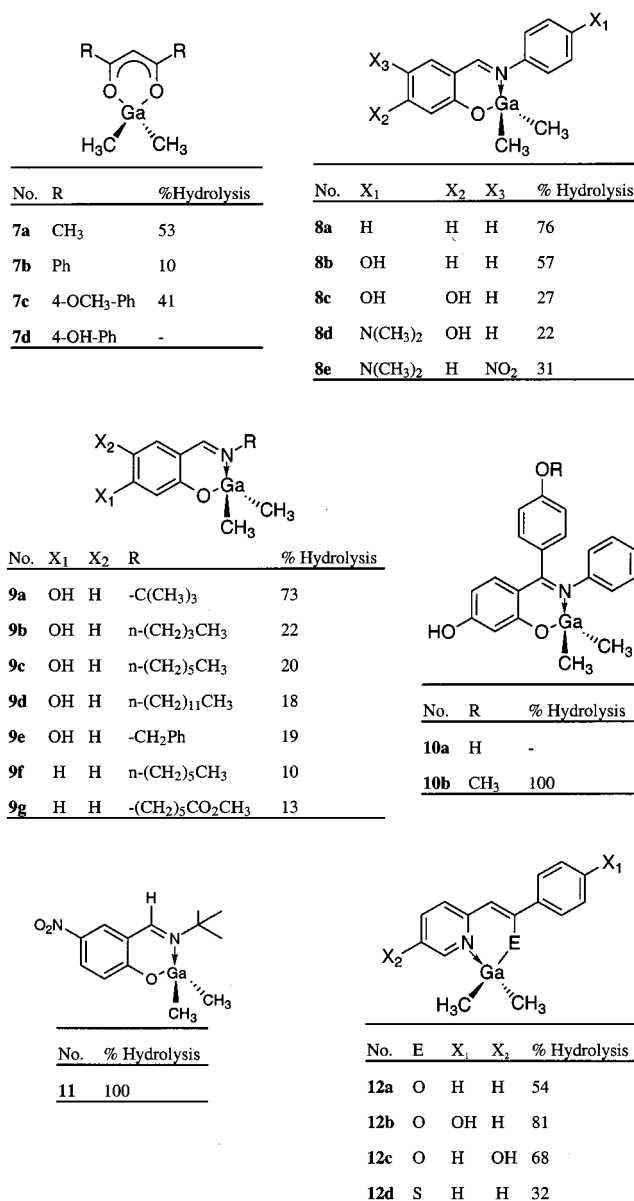(13) Katzenellenbogen, J. A. In *Estrogens, Progestins, and Their Antagonists*; Pavlik, E. J., Ed.; Birkhäuser: Boston, 1996; p 197.
(14) Harris, W. R.; Pecoraro, V. L. *Biochemistry* **1983**, *22*, 292.

No.	R
1a	CH$_3$
1b	Ph
1c	4-OCH$_3$-Ph
1d	4-OH-Ph

No.	X$_1$	X$_2$	X$_3$
2a	H	H	H
2b	OH	H	H
2c	OH	OH	H
2d	N(CH$_3$)$_2$	OH	H
2e	N(CH$_3$)$_2$	H	NO$_2$

R = -CH$_2$...CH$_3$
1' n'

No.	X	R
3a	OH	-C(CH$_3$)$_3$
3b	OH	n-(CH$_2$)$_3$CH$_3$
3c	OH	n-(CH$_2$)$_5$CH$_3$
3d	OH	n-(CH$_2$)$_{11}$CH$_3$
3e	OH	-CH$_2$Ph
3f	H	n-(CH$_2$)$_5$CH$_3$
3g	H	-(CH$_2$)$_5$CO$_2$CH$_3$

No.	R
4a	H
4b	OCH$_3$

No.	E
5a	O
5b	S

No.	E	X$_1$	X$_2$
6a	O	H	H
6b	O	OH	H
6c	O	H	OH
6d	S	H	H

Figure 1. Ligand precursors.

No.	R	%Hydrolysis
7a	CH$_3$	53
7b	Ph	10
7c	4-OCH$_3$-Ph	41
7d	4-OH-Ph	-

No.	X$_1$	X$_2$	X$_3$	% Hydrolysis
8a	H	H	H	76
8b	OH	H	H	57
8c	OH	OH	H	27
8d	N(CH$_3$)$_2$	OH	H	22
8e	N(CH$_3$)$_2$	H	NO$_2$	31

No.	X$_1$	X$_2$	R	% Hydrolysis
9a	OH	H	-C(CH$_3$)$_3$	73
9b	OH	H	n-(CH$_2$)$_3$CH$_3$	22
9c	OH	H	n-(CH$_2$)$_5$CH$_3$	20
9d	OH	H	n-(CH$_2$)$_{11}$CH$_3$	18
9e	OH	H	-CH$_2$Ph	19
9f	H	H	n-(CH$_2$)$_5$CH$_3$	10
9g	H	H	-(CH$_2$)$_5$CO$_2$CH$_3$	13

No.	R	% Hydrolysis
10a	H	-
10b	CH$_3$	100

No.	% Hydrolysis
11	100

No.	E	X$_1$	X$_2$	% Hydrolysis
12a	O	H	H	54
12b	O	OH	H	81
12c	O	H	OH	68
12d	S	H	H	32

Figure 2. Structure of gallium complexes and percent hydrolysis (after 12−24 h with 1000-fold excess of water in acetone-d_6 monitored by ^{1}H NMR).

Ga$^+$, a cation in which the metal−carbon bonds are highly stable toward hydrolysis.[1,16] The charge and size of this cation apparently make it sufficiently dissimilar to Fe^{3+} to prevent significant binding by plasma proteins.[16] Low affinity for plasma proteins, a tetracoordinate (rather than hexacoordinate) geometry, and the alkyl ligand environment of the metal suggest that dimethylgallium compounds may be more adaptable to the design of ligands for biological receptors than are multidentate Ga^{3+} complexes.

The goal of this investigation was to prepare a number of tetracoordinate compunds in which the (CH$_3$)$_2$Ga moiety is complexed with a bidentate Lewis base and to examine what structural factors affect the stability of these complexes toward decomplexation of the stable (CH$_3$)$_2$Ga moiety in the presence of water (i.e., hydrolysis) to determine whether complexes that are stable to hydrolysis can be prepared. Developing stable
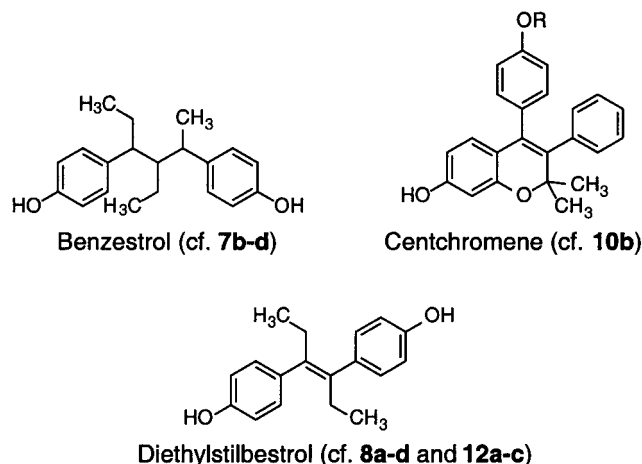
gallium−heteroatom bonds rather than stable gallium−carbon bonds proved to be the challenge in this endeavor.

Results and Discussion

Preparation of Ligands and Dimethylgallium Compounds. The six classes of ligands and the six classes of dimethylgallium compounds prepared from them are shown in Figures 1 and 2, respectively. The β-diketonate ligands (**1a−d**) and their corresponding complexes (**7a−d**) represent species with two oxygen donor atoms. The *N*-alkylaldimines (**2a−e**, **5** and **8a−e**, **11**), *N*-arylaldimines (**3a−g** and **9a−g**), and the related *N*-arylbenzophenonimine analogues (**4a,b** and **10a,b**) are all representatives of N,O-bidentate complexes. Finally, the α-(2-pyridyl)acetophenones and thioacetophenones (**6a−d** and **12a−d**) provide an alternate N,O- and in one case an N,S-chelation geometry. As is mentioned below, the design of several of these

(15) Sun, Y.; Andersen, C. J.; Pajeau, T. S.; Reichert, D. E.; Hancock, R. D.; Motekaitis, R. J.; Martell, A. E.; Welch, M. J. *J. Med. Chem.* **1996**, *39*, 458.
(16) Coggin, D. K.; Mathias, C. J.; Green, M. L. *Nucl. Med. Biol.* **1994**, *21*, 283.
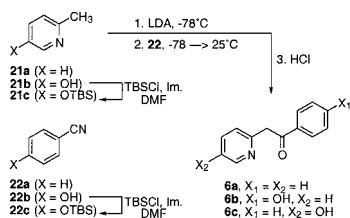
Benzestrol (cf. 7b-d)

Centchromene (cf. 10b)

Diethylstilbestrol (cf. 8a-d and 12a-c)

Figure 3. Classes of nonsteroidal estrogens related to dimethyl gallium complexes.

Table 1. Preparation of Gallium Complexes

	ligand		$(CH_3)_2GaOH$			
no.	mass (mg)	mmol	mass (mg)	mmol	excess (%)	yield (%)
7c	81.3	0.29	35.4	0.30	6	84
7d	23.2	0.09	11.1	0.10	11	74
8a	84.6	0.43	52.7	0.45	6	97
8	81.2	0.38	46.7	0.40	5	100
8d	131.1	0.57	115.3	0.99	70	97
8e	94.8	0.33	63.2	0.54	63	85
9	61.4	0.32	39.4	0.34	6	100
9b	71.7	0.37	45.9	0.39	6	95
9c	72.7	0.33	40.0	0.34	4	92
9d	81.2	0.27	32.4	0.28	5	96
9e	81.8	0.36	45.2	0.39	8	86
9f	64.0	0.31	38.0	0.33	5	100
9g	40.0	0.18	22.0	0.19	4	95
10a	71.6	0.23	28.8	0.25	6	85
10b	122.0	0.38	71.4	0.62	60	76
11	76.1	0.34	42.2	0.36	6	78
12a	115.0	0.58	73.0	0.62	7	97
12b	104.0	0.49	61.0	0.52	6	92
12c	200.0	0.94	117.0	0.99	5	91
12d	50.0	0.23	29.0	0.25	9	89

Scheme 1. Synthesis of α-(2-Pyridyl)acetophenones

21a (X = H)
21b (X = OH)
21c (X = OTBS)

22a (X = H)
22b (X = OH)
22c (X = OTBS)

6a, $X_1 = X_2 = H$
**6b**, $X_1 = OH$, $X_2 = H$
6c, $X_1 = H$, $X_2 = OH$

gallium compounds was inspired by the structure of certain nonsteroidal ligands for the estrogen receptor (Figure 3). The synthesis of the ligands followed literature precedent or was accomplished using well-precedented methods for aromatic substitution and imine formation reactions. Procedures for the synthesis of new compounds are presented in detail in the Experimental Section and in Scheme 1 and will not be discussed further. The reaction scale and yield of complex formation are given in Table 1.

By all structural comparisons, the dimethylgallium complexes **7**–**12** are similar to reported compounds. Crystal structures of two of the compounds, the β-diketonate **7c** (Figure 4) and the α-(2-pyridyl)acetophenone
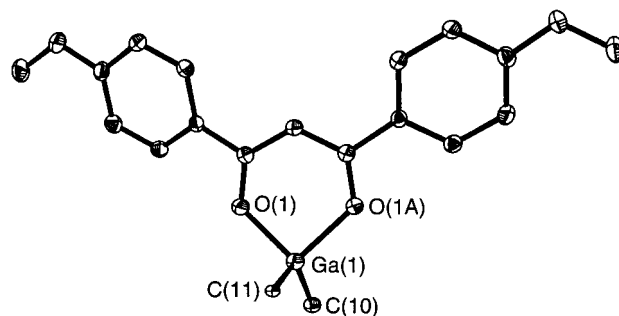
Figure 4. ORTEP plot of β-diketonate compound **7c** with thermal ellipsoids at 35%.
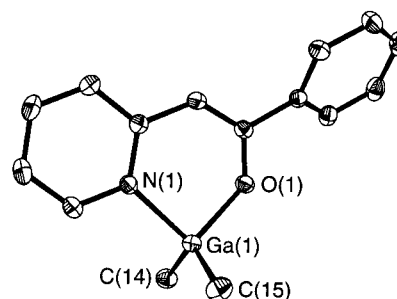
Figure 5. ORTEP plot of α-(2-pyridyl)acetophenone **12a** with thermal ellipsoids at 35%.

12a (Figure 5), confirm a four-coordinate environment about the metal and bond lengths to gallium that are similar to those in other known complexes; details are given in Tables 3 and 4.[17] Reflecting the electropositive character of the metal center, NMR spectra of the compounds consistently show the dimethylgallium hydrogens and carbons slightly upfield of TMS. There is, however, remarkably little difference between NMR spectra of the gallium complexes and those of the free ligand and dimethylgallium hydroxide itself. The ^1H NMR resonances of the methyl groups in dimethylgallium hydroxide (δ −0.48) appear at somewhat lower field in the complexes (ca. δ −0.46), the shift in the resonance position of these methyl groups upon hydrolysis of the complex being generally 0.03 ppm downfield. Similarly, the resonances for most of the aromatic and vinylic protons in these systems appear at somewhat higher field in the complexes than in the free ligands; again, the shift is small, ca. 0.05−0.15 ppm. Mass spectra show a peak for the molecular ion (M$^+$) or, more commonly, the mass peak resulting from monodemethylation at the gallium center. In either case, the mass peaks corresponding to the two stable isotopes of gallium (^{69}Ga and ^{71}Ga) show the expected relative intensities of 3:2.

Hydrolysis Studies. There are reports that the stability of *trialkylgallium* complexes toward hydrolysis can be improved by intramolecular chelation.[18,19] There are also qualitative reports of the hydrolytic stability of *dimethylgallium* compounds of the type we studied. For example, dimethylgallium complexes of substituted salicylideneimine and dimethylaminomethyl-3-pyridol-

(17) Schumann, H.; Hartmann, U.; Dietrich, A.; Pickardt, J. *Angew. Chem., Int. Ed. Engl.* **1988**, *27*, 1077.
(18) Schumann, H.; Hartmann, U.; Wasserman, W. *Polyhedron* **1990**, *9*, 353.
(19) Schumann, H.; Hartmann, U.; Wassermann, W.; Dietrich, A.; Gorlitz, F.; Pohl, L.; Hostalek, M. *Chem. Ber.* **1990**, *123*, 2093.

Table 2. Crystallographic Details

complex	7c	12a
empirical formula	$C_{19}H_{21}GaO_4$	$C_{15}H_{16}GaNO$
fw	383.08	296.01
temp	198(2) K	198(2) K
wavelength	0.710 73 Å	0.710 73 Å
cryst syst	orthorhombic	monoclinic
space group	Pnma	$P2_1/n$
unit cell dimens	$a = 7.915$ Å	$a = 9.3261(2)$ Å
	$b = 21.0640(4)$ Å	$b = 11.6182(2)$ Å
	$c = 10.5510(2)$ Å	$c = 12.9708(3)$ Å
volume	1759.08(5) Å^3	1369.14(5) Å^3
Z	4	4
density, calcd	1.446 g cm^{-3}	1.436 g cm^{-3}
abs coeff	1.583 mm^{-1}	1.997 mm^{-1}
no. of indep reflns	10688 (R(int) = 0.0384)	8701 (R(int) = 0.0533)
refinement method	full matrix least-squares on F^2	full matrix least-squares on F^2
no. of data/restraints/params	2213/0/115	3297/0/163
goodness-of-fit (GoF) on F^2	1.101	1.124
final R indices ($I > 2\sigma(I)$)	R1 = 0.0518, wR2 = 0.1420	R1 = 0.0334, wR2 = 0.0652
R indices (all data)	R1 = 0.0635, wR2 = 0.1536	R1 = 0.0496, wR2 = 0.0744

Table 3. Selected Bond Distances and Angles for β-Diketonate Complex 7c

Bond Distances (Å)	
Ga(1)−O(1)	1.921(2)
Ga(1)−C(10)	1.959(4)
Ga(1)−C(11)	2.004(3)

Bond Angles (deg)	
O(1)−Ga(1)-O(1A)	93.89(14)
O(1)−Ga(1)-C(10)	108.88(12)
O(1)−Ga(1)-C(11)	106.43(10)
C(10)−Ga(1)-C(11)	127.2(2)
C(8)−O(1)-Ga(1)	124.4(2)

Table 4. Selected Bond Distances and Angles for α-(2-Pyridyl)Acetophenone Complex 12a

Bond Distances (Å)			
Ga(1)−O(1)	1.899(2)	Ga(1)−C(15)	1.960(3)
Ga(1)−C(14)	1.958(3)	Ga(1)−N(1)	2.027(2)

| Bond Angles (deg)			
O(1)−Ga(1)-C(14)	108.99(10)	C(15)−Ga(1)-N(1)	106.40(10)
O(1)−Ga(1)-C(14)	109.78(10)	C(1)−N(1)-Ga(1)	117.4(2)
C(14)−Ga(1)-C(15)	125.71(11)	C(5)−N(1)-Ga(1)	123.3(2)
O(1)−Ga(1)-N(1)	94.10(7)	C(7)−O(1)-Ga(1)	124.0(2)
C(14)−Ga(1)-N(1)	107.13(10)		

ato ligands are described as "air and moisture sensitive"[20,21] or "air stable", respectively.[20,21]

In some quantitative hydrolysis studies of trialkylgallium or dialkylphosphidogallium compounds, the reaction of the complex with small amounts (usually 1 equiv) of water was studied. Aggregated dialkylgallium hydroxides are produced by these reactions.[22−24] Our experiments were similar, in that $[(CH_3)_2GaO]_n$ was the observed product of hydrolysis; however, our experiments were designed to allow quantitative comparisons of hydrolytic stability in screening for potential radiopharmaceuticals. Thus, in contrast to this earlier work, we added a relatively large quantity of water (1000 equiv) to the gallium compound. Also, the hydroxide product resulted from addition of water across the *Ga−*

(20) Chong, K. S.; Rettig, S. J.; Storr, A.; Trotter, J. *Can. J. Chem.* **1977**, *55*, 2540.
(21) Onyiriuka, E. C.; Rettig, S. J.; Storr, A.; Trotter, J. *Can. J. Chem.* **1987**, *65*, 782.
(22) Power, M. B.; Cleaver, W. M.; Apblett, A. W.; Barron, A. A. *Polyhedron* **1992**, *11*, 477.
(23) Naiini, A. A.; Young, V.; Han, Y.; Akinc, M.; Verkade, J. G. *Inorg. Chem.* **1993**, *32*, 3781.
(24) Atwood, D. A.; Cowley, A. H.; Harris, P. R.; Jones, R. A.; Koschmieder, S. U.; Nunn, C. M. *Organometallics* **1993**, *12*, 24.

heteroatom bond in our dimethylgallium complexes, rather than from hydrolysis of a *Ga−carbon bond* in a trialkyl gallium compound.

Because it can be monitored by ^{1}H NMR, the hydrolysis process can be conveniently followed. Hydrolysis appears to be relatively rapid, and in the cases where the kinetics were followed in some detail, it reached a limiting value within a few hours. So, the extent of hydrolysis was routinely measured after 12−24 h, at which point it had reached an equilibrium value. Because the hydrolysis assay was done at a fixed concentration of dimethylgallium complex (200 mM, see Experimental Section) and a fixed, 1000-fold excess of water, we are measuring the *relative thermodynamic stabilities* of these complexes. The results of the hydrolysis studies on the complexes **7−12** are summarized in Figure 2.

β-Diketonate Compounds 7a−7c. Complexes of this structure were inspired by certain nonsteroidal ligands for the estrogen receptor of the benzestrol class (see Figure 3). Hydrolysis studies on these complexes demonstrated how chelate structure affected hydrolytic stability (see Figure 2). The fact that the published synthesis of **7a** involves an extraction of excess acetylacetonate with a water/diethyl ether system makes $(CH_3)_2Ga(acac)$ appear stable to hydrolysis. By contrast, our measurements show that, in acetone, $(CH_3)_2Ga$-(acac) is more than 50% hydrolyzed by 1000 equiv of water. These observations can be reconciled by the equilibrium

$$(CH_3)_2Ga(acac) + H_2O \rightleftharpoons (CH_3)_2GaOH + acacH$$
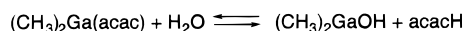
Preferential solubility of $(CH_3)_2Ga(acac)$ in ether and removal of water by bulk partitioning and chemical drying would explain how the unstable $(CH_3)_2Ga(acac)$ can be prepared using an aqueous workup. A second implication of our results is that the in vivo distribution of $[^{67}Ga](CH_3)_2Ga(acac)$ is probably largely controlled by its hydrolysis product, $[^{67}Ga](CH_3)_2GaOH$.

With identical heteroatom donors, the β-diketonate complexes **7** are a simple model for probing the differences in hydrolytic stability that can result from structural changes distal to the metal (see Figure 2). Electronic influences are most obvious in explaining the relative stabilities of **7a** vs **7b**. Replacing the methyl

group in **7a** with the more electron-withdrawing phenyl groups in **7b** lowers the basicity and thereby reduces the reactivity of the complexed ligand toward water. Addition of electron-donating methoxy groups in **7c** partially reverses the decrease in basicity and, therefore, increases hydrolytic stability.

N-Arylaldimine Compounds (8a−e). The structure of this class of gallium compounds was inspired by the structure of the nonsteroidal estrogens of the stilbestrol class (see Figure 3). These complexes were the first system in which we separately tuned the basicities of the two different donor atoms of the ligand. Specifically, we designed a series to increase the basicity of the N-donor and decrease the basicity of the O-donor in an attempt to maximize ligand affinity for $(CH_3)_2$-Ga^+ and minimize reactivity of the dimethylgallium complex toward water. Implementing this trend with substituents generally increased the hydrolytic stability of the compounds (**8a−d**) as desired (see Figure 2). In this series, we used hydroxyl substituents to alter donor atom basicity because estrogenicity, a target property, is often engendered by the phenolic OH functionality.[25] The fact that the most acidic oxygen donor ligand (**8e**, bearing a nitro group) did not have the greatest hydrolytic stability suggests that a maximum desirable acidity can be exceeded and that in this ligand the σ-donor character of the oxygen donor toward $(CH_3)_2Ga^+$ was diminished.

N-Alkylaldimine Compounds (9a−g). The hydrolytic behavior of these complexes is significant because of the emergence of a new parameter influencing hydrolytic stability. The large hydrolytic labilizing effect of substituting a *tert*-butyl group (**9a**) for an *n*-butyl group (**9b**) is evidence that the bulk of a substituent on the imine nitrogen can compromise hydrolytic stability (see Figure 2). This effect may reflect the relative thermodynamic stabilities of the two complexes. The length of an *n*-alkyl chain, however, had little effect on the reactivity of these compounds (**9b−e**) toward water. Removal of the meta hydroxyl group (**9f**) afforded the most hydrolytically stable member of the series. Addition of an aryl (**9e**) or ester (**9g**) functionality at the ω-carbon did not significantly affect the hydrolytic stability of these complexes.

Approximately the same range of hydrolytic stability is present across series **8** and **9**, but *N*-(*n*-alkyl) groups in complexes **9** stabilize the complexes more than does an unsubstituted *N*-phenyl group in complexes **8**. This difference probably parallels basicity differences at the imine nitrogen. Why a meta OH group should have opposite results on hydrolytic stability in the two series is not clear, however: **8c** (with a *m*-OH) is more stable than **8b**, whereas **9a** (with a *m*-OH) is less stable than **9f**. If these complexes are being stabilized against hydrolysis by formation of micellar structures in which the Ga−O bonds are being sequestered away from water where they are selectively protected from hydrolysis, then micellar destabilization by a polar substituent on the aromatic ring would be understandable.

N-Aryl−Hydroxybenzophenonimine Compounds (10a and 10b). These compounds were prepared because of their similarity to centchromene-type estro-

gens (see Figure 3). The marked hydrolytic instability of **10b** is significant by comparison with that of **8b**. Replacement of the aldimine hydrogen (of **8b**) with a *p*-methoxyphenyl group (as in **10b**) would be expected to reduce the basicity of the imine nitrogen and, consequently, the donor character of the ligand toward $(CH_3)_2Ga^+$, increasing its stability, as was observed. Steric crowding in this complex is also expected to twist this phenyl substituent largely out of conjugation with the aldimine.

Compound 11. Complex **11** could be considered in the class of *N*-alkylaldimine complexes (**9**), but was studied separately, for comparative purposes. The low hydrolytic stability of complex **11** is consistent with two earlier observations: (a) the steric crowding caused by a *N*-(*tert*-butyl) group (as in complex **9a**) and (b) the (apparently) low donor character of the *p*-nitrophenoxide ligand (as in complex **8e**). Improvement in stability through a better match of acid/base softness was probed by substituting sulfur for oxygen. We found, however, that the S-donor complex could not be formed from the free thiophenol (**5b**) and $(CH_3)_2GaOH$, even in refluxing THF. The sulfur atom may be sufficiently larger than oxygen to cause significant strain in the incipient six-member ring that includes the $(CH_3)_2Ga^+$ moiety.

α-Pyridylacetophenone and Thioacetophenone Compounds (12a-d). This system, which provides an alternate geometry for bidentate complexation of the dimethylgallium cation, was systematically modified using hydroxyl groups to probe the effect of increasing the basicity of the N-donor and decreasing the basicity of the O-donor (as was done in the series **8a−d**), in an attempt to maximize ligand affinity for $(CH_3)_2Ga^+$ and minimize the reactivity of the complex toward water. However, in contrast to the results in the **8a−d** series, a marked decrease in hydrolytic stability was observed with increasing basicity of the O-donor and decreasing basicity of the N-donor (**12b** and **12c** vs **12a**). Substituting the O-donor for an S-donor increased the acidity of the ligand and hence its σ-donor ability toward $(CH_3)_2$-Ga^+, affording a somewhat greater stability to this complex (**12d**) than to its oxygen congener (**12a**). The differences in the response of the hydrolytic stability of the dimethylgallium compounds in the series **8a−d** and **12a−c** to hydroxyl substitution could be due to the different paths of conjugation between the hydroxyl groups and the N-, and O-donor atoms in the two complexes, as their structures are rather different.

Conclusion

We have shown that four-coordinate dimethylgallium compounds exhibit marked differences in their hydrolytic stability in the presence of 1000-fold excess of water. In our model systems, stability of substituted salicylideneimine complexes was favored by basicity and steric accessibility of the imine nitrogen. Stability decreased when the acidity of the phenolic oxygen was increased by a *p*-nitro group. Sulfur donor complexes showed only marginal improvement in stability relative to O-donor analogues.

Future efforts to develop hydrolytically stable dimethylgallium complexes as radiopharmaceuticals should concentrate on ligands different from those we have described. Alternatives include five-coordinate gallium

(25) Anstead, G. M.; Carlson, K. E.; Katzenellenbogen, J. A. *Steroids* **1997**, *62*, 268.

compounds and dialkyl compounds in which the pharmacophore is included in the alkyl group(s). In this regard, it is of note that none of the dimethylgallium complexes underwent hydrolytic scission of the gallium−alkyl bond.

Experimental Section

Ligand Synthesis. Compounds **1a**, **1b**, and **2a** were purchased from Sigma-Aldrich. Published procedures were employed to synthesize **1c**,[26,27] **2b**,[28] **2c**,[29] and **5b**.[30] Other ligand precursors (**1d**, **2de**, **3a−g**, **4a,b**, **6a−d**, **21c**, **22c**) were synthesized by the methods described in the Supporting Information.

Gallium Complexes. General Procedure for Formation of Gallium Complexes. Dimethylgallium hydroxide and complex **7a** were prepared by a published procedure.[31,32] Except where otherwise noted, the remaining gallium complexes were prepared as follows. A 2 mL flask was charged with 70−125 mg of ligand precursor, a 5−8% molar excess (of 1:1 stoichiometry) of $(CH_3)_2GaOH$, and 0.5−0.7 mL of THF. The resulting solution was stirred 8−12 h; then $MgSO_4$ was added, and the mixture was stirred an additional 10 min. Filtration through Celite afforded a clear filtrate from which solvent was removed in vacuo to afford a solid. Since the complexes proved unstable on alumina, silica, and C18 silica, they were washed with three 5 mL portions of boiling petroleum ether to remove excess $(CH_3)_2GaOH$ and dried in vacuo. Compounds **9f** and **9g** were soluble in petroleum ether; they were characterized with 4−5% excess $(CH_3)_2GaOH$ present.

κ^2O,O-Dibenzoylmethanolatodimethylgallium (7b). To 0.53 g (5.21 mmol) of $(CH_3)_2GaOH$ dissolved in 5 mL of (1:1:1) benzene/hexane/Et$_2$O was added a solution of 1.17 g (5.21 mmol) of dibenzoylmethane in 7 mL of benzene. The solution was stirred for 12 h at 22 °C. Removal of solvent in vacuo afforded a solid that was subsequently recrystallized from hexane to afford yellow needles. Yield: 0.38 g (22%). Additional product was obtained by concentration of the mother liquor. ^{1}H NMR (acetone-d_6): δ 8.14 (d, 4H, J = 7.1 Hz), 7.62−7.51 (m, 6H), 7.06 (s, 1H), −0.16 (s, 6H). ^{13}C NMR (acetone-d_6): δ 186.8, 138.5, 133.5, 129.5, 129.4, 129.2, 128.6, 128.1, 123.1, −6.8. LRMS (EI): M − CH$_3^+$ = 307. Anal. Calcd for C$_{17}$H$_{17}$O$_2$Ga: C, 63.21; H, 5.30. Found: C, 62.84; H, 5.11.

κ^2O,O-1,3-Bis(4-methoxyphenyl)propane-1,3-dionolatodimethylgallium (7c). ^{1}H NMR (CDCl$_3$): δ 7.95 (d, 4H, J = 9.4 Hz), 6.92 (d, 4H, J = 8.8 Hz), 6.64 (s, 1H), 3.88 (s, 6H), −0.17 (s, 6H). ^{13}C NMR (CDCl$_3$): δ 184.5, 163.3, 130.8, 130.6, 129.9, 114.3, 114.0, 92.5, 55.7, −6.5. LRMS (EI): M − CH$_3^+$ = 367. Anal. Calcd for C$_{19}$H$_{21}$O$_4$Ga: C, 59.57; H, 5.33. Found: C, 59.66; H, 5.40.

κ^2O,O-1,3-Bis(4-hydroxyphenyl)propane-1,3-dionolatodimethylgallium (7d). ^{1}H NMR (acetone-d_6): δ 9.18 (s, 2H), 8.04 (d, 4H, J = 8.8 Hz), 6.94 (d, 4H, J = 8.8 Hz), 6.91 (s, 1H), −0.25 (s, 6H). ^{13}C NMR (acetone-d_6): δ 184.9, 162.5, 130.9, 130.0, 123.2, 116.1, 92.2, −7.0. LRMS (EI): M − CH$_3^+$ = 339. Anal. Calcd for C$_{17}$H$_{17}$O$_4$Ga: C, 57.51; H, 4.82. Found: C, 57.16; H, 4.40.

κ^2N,O-2-Phenyliminomethylphenolatodimethylgallium (8a). ^{1}H NMR (acetone-d_6): δ 8.60 (s, 1H), 7.58 (dd, 1H, J = 8.4, 8.4 Hz), 6.83 (d, 1H, J = 8.5 Hz), 6.76 (ddd, 1H, J = 7.3, 7.3, 1.0 Hz), −0.26 (s, 6H). ^{13}C NMR (acetone-d_6): δ 169.8, 168.2, 148.0, 137.8, 137.4, 130.6, 130.3, 128.5, 123.0, 122.6, 122.0, 119.7, 116.9, −6.4. LRMS (EI): M − CH$_3^+$ = 280. HRMS (EI) M$^+$ Calcd for C$_{15}$H$_{16}$NOGa: 295.0488. Found: 295.0487.

κ^2N,O-2-[(4-Hydroxyphenylimino)methyl]phenolatodimethylgallium (8b). ^{1}H NMR (acetone-d_6): δ 8.78 (s, 1H), 8.52 (s, 1H), 7.43 (d, 1H, J = 7.8 Hz), 7.38 (dd, 1H, J = 6.8, 6.8 Hz), 7.29 (d, 2H, J = 8.8 Hz), 6.98 (d, 2H, J = 8.8 Hz), 6.77 (d, 1H, J = 8.5 Hz), 6.71 (dd, 1H, J = 7.4, 7.4 Hz). ^{13}C NMR (acetone-d_6): δ 167.3, 167.0, 157.3, 139.4, 136.5, 136.4, 123.0, 122.1, 119.1, 116.4, 116.1, −7.1. LRMS (EI): M − CH$_3^+$ = 296. HRMS (EI) M − CH$_3^+$ Calcd for C$_{13}$H$_{11}$NO$_2$: 296.0202. Found: 296.0204.

κ^2N,O-4-[(4-Hydroxyphenylimino)methyl]benzene-1,3-diolatodimethylgallium (8c). ^{1}H NMR (1:4 CD$_3$OD/acetone-d_6): δ 8.31 (s, 1H), 7.24 (d, 1H, J = 8.6 Hz), 7.17 (d, 2H, J = 8.9 Hz), 6.89 (d, 1H, J = 9.0 Hz), 6.24 (dd, 1H, J = 10.0, 2.0 Hz), 6.17 (d, 1H, J = 2.7 Hz), −0.26 (s, 6H). ^{13}C NMR (acetone-d_6): δ 169.9, 166.2, 157.4, 140.4, 139.2, 123.5, 117.0, 113.9, 107.4, 106.9, −6.4. LRMS (EI): M − CH$_3^+$ = 312. HRMS (EI) M$^+$ Calcd for C$_{15}$H$_{16}$NO$_3$Ga: 327.0386. Found: 327.0382.

κ^2N,O-4-[(4-*N,N*-Dimethylaminophenylimino)methyl]benzene-1,3-diolatodimethylgallium (8d). ^{1}H NMR (acetone-d_6): δ 8.33 (s, 1H), 7.27 (d, 1H, J = 8.5 Hz), 7.22 (d, 2H, J = 8.8 Hz), 6.82 (d, 2H, J = 8.8 Hz), 6.28 (dd, 1H, J = 8.5, 2.2 Hz), 6.20 (s, 1H), 3.01 (s, 6H), −0.34 (s, 6H). ^{13}C NMR (acetone-d_6): δ 169.1, 163.9, 149.9, 138.2, 136.6, 122.1, 113.3, 112.9, 106.5, 106.2, 39.8, −7.1. LRMS (EI): M − CH$_3^+$ = 339. Anal. Calcd for C$_{17}$H$_{21}$N$_2$O$_2$Ga: C, 57.20; H, 5.96; N, 7.89. Found: C, 57.49; H, 6.14; N, 7.59.

κ^2N,O-2-[(4-*N,N*-Dimethylaminophenylimino)methyl]-4-nitrophenolatodimethylgallium (8e). ^{1}H NMR (acetone-d_6) δ 8.81 (s, 1H), 8.53 (d, 1H, J = 2.9 Hz), 8.20 (dd, 1H, J = 9.2, 2.9 Hz), 7.41 (d, 1H, J = 9.0 Hz), 6.87 (d, 1H, J = 9.0 Hz), 6.87 (d, 1H, J = 9.0 Hz), 3.04 (s, 6H), −0.23 (s, 6H). ^{13}C NMR (acetone-d_6) δ 123.4, 123.2, 113.4, 40.3, −6.1. LRMS (EI) M-CH$_3^+$ = 368. HRMS (EI) M$^+$ Calcd for C$_{17}$H$_{21}$N$_3$O$_3$Ga: 387.0760. Found: 387.0761.

κ^2NO-4-*tert*-Butyliminomethylbenzene-1,3-diolatodimethylgallium (9a). ^{1}H NMR (acetone-d_6): δ 8.34 (s, 1H), 7.17 (d, 1H, J = 8.6 Hz), 6.21 (dd, 1H, J = 8.5, 2.0 Hz), 6.14 (d, 1H, J = 1.8 Hz), 1.43 (s, 9H), −0.34 (s, 6H). ^{13}C NMR (acetone-d_6): δ 172.8, 169.2, 166.3, 138.7, 137.7, 113.3, 106.6, 60.1, −4.0. LRMS (EI): M − CH$_3^+$ = 276. HRMS (EI) M$^+$ Calcd for C$_{13}$H$_{20}$NO$_2$Ga: 291.0750. Found: 291.0751.

κ^2N,O-4-*n*-Butyliminomethylbenzene-1,3-diolatodimethylgallium (9b). ^{1}H NMR (acetone-d_6): δ 8.21 (s, 1H), 7.14 (d, 1H, J = 8.5 Hz), 6.25 (dd, 1H, J = 8.5, 2.2 Hz), 6.19 (d, 1H, J = 2.0 Hz), 3.59 (t, 2H, J = 7.6 Hz), 1.70 (tt, 2H, J = 7.3, 7.3 Hz), 1.41 (tt, 2H, J = 7.5, 7.5 Hz), 0.98 (t, 3H, J = 4.2 Hz), −0.37 (s, 6H). ^{13}C NMR (acetone-d_6): δ 169.5, 169.1, 138.0, 113.0, 106.9, 106.6, 58.4, 32.9, 20.5, 13.9, −7.0. LRMS (EI): M − CH$_3^+$ = 276. HRMS (EI) M$^+$ calcd for C$_{13}$H$_{20}$NO$_2$Ga: 291.0750. Found: 291.0748.

κ^2N,O-4-*n*-Hexyliminomethylbenzene-1,3-diolatodimethylgallium (9c). ^{1}H NMR (acetone-d_6): δ 8.18 (s, 1H), 7.10 (d, 1H, J = 8.6 Hz), 6.21 (dd, 1H, J = 8.4, 2.4 Hz), 6.16 (d, 1H, J = 2.4 Hz), 3.56 (t, 2H, J = 6.4 Hz), 1.65 (tt, 2H, J = 7.1, 7.1 Hz), 1.32−1.34 (m 6H), 0.89 (t, 3H, J = 7.1 Hz), −0.34 (s, 6H). ^{13}C NMR (acetone-d_6): δ 169.5, 169.1, 165.5, 138.0, 113.0, 107.0, 106.7, 58.7, 32.1, 30.9, 27.0, 23.1, 14.2, −7.0. LRMS (EI): M − CH$_3^+$ = 304. HRMS (EI) M − CH$_3^+$ calcd for C$_{14}$H$_{21}$NO$_2$Ga: 304.0828. Found: 304.0827.

κ^2N,O-4-Dodecyliminomethylbenzene-1,3-diolatodimethylgallium (9d). ^{1}H NMR (acetone-d_6): δ 8.16 (s, 1H), 7.10 (d, 1H, J = 8.5 Hz), 6.21 (dd, 1H, J = 8.4, 2.4 Hz), 6.17 (d, 1H, J = 2.4 Hz), 3.55 (t, 2H, J = 7.6 Hz), 1.68 (m, 2H), 1.35−1.20 (m, 18H), 0.88 (t, 3H, J = 6.4 Hz), −0.40 (s, 6H). ^{13}C NMR (acetone-d_6): δ 169.4, 169.0, 165.4, 137.9, 113.0, 107.0, 106.7, 58.7, 32.6, 30.8, 30.3, 30.1, 27.3, 23.3, 14.3, −6.9.

(26) Adams, J. T.; Hauser, C. R. *J. Am. Chem. Soc.* **1944**, *66*, 1220.
(27) Levine, R.; Conroy, J. A.; Adams, J. T.; Hauser, C. R. *J. Am. Chem. Soc.* **1945**, *67*, 1510.
(28) Haegle, E. *Chem. Ber.* **1892**, *25*, 2753.
(29) Helfrich, B.; Mitrowsky, A. *Chem. Ber.* **1952**, *85*, 1.
(30) Korobov, M. S.; Minkin, V. I. *J. Org. Chem. USSR* **1975**, *11*, 826.
(31) Coates, G. E.; Hayter, R. G. *J. Chem. Soc.* **1953**, 2519.
(32) Tobias, R. S.; Sprague, M. J.; Glass, G. E. *Inorg. Chem.* **1968**, *7*, 1714.

LRMS (EI): M − CH$_3$+ = 388. HRMS (EI) M+ calcd for C$_{21}$H$_{36}$-NO$_2$Ga: 403.2002. Found: 403.2003.

κ²*N*,*O*-4-Benzyliminomethylbenzene-1,3-diolatodimethylgallium (9e). ^{1}H NMR (acetone-d_6): δ 8.39 (s, 1H), 7.39−7.34 (m, 5H), 7.17 (d, 1H, J = 8.5 Hz), 6.24 (d, 1H, J = 8.5 Hz), 6.15 (d, 1H, J = 2.0 Hz), 4.74 (s, 2H), −0.67 (s, 6H). ^{13}C NMR (acetone-d_6): δ 169.8, 169.4, 138.3, 137.1, 129.8, 129.5, 128.9, 113.1, 106.9, 106.8, 62.4, −7.2. LRMS (EI): M − CH$_3$+ = 310. HRMS (EI) calcd for C$_{15}$H$_{15}$NO$_2$Ga: 310.0359. Found: 310.0358.

κ²*NO*-2-*n*-Hexyliminomethylphenolatodimethylgallium (9f). ^{1}H NMR (acetone-d_6): δ 8.37 (s, 1H), 7.31 (ddd, 1H, J = 8.0, 8.0, 2.0 Hz), 7.26 (dd, 1H, J = 7.8, 2.0 Hz), 6.71 (d, 1H, J = 8.4 Hz), 6.64 (ddd, 1H, J = 8.0, 8.0, 1.0 Hz). ^{13}C NMR (acetone-d_6): δ 170.5, 167.4, 136.4, 136.0, 122.7, 119.2, 116.4, 59.1, 32.0, 30.6, 27.0, 23.1, 14.2, −6.9. LRMS (EI): M − CH$_3$+ = 288. HRMS (EI) M+ calcd for C$_{21}$H$_{36}$NO$_2$Ga: 303.1114. Found: 303.1117.

κ²*N*-2-[(6-Methoxycarbonylhexylimino)methyl]phenolatodimethylgallium (9g). ^{1}H NMR (acetone-d_6): δ 8.37 (s, 1H), 7.31 (ddd, 1H, J = 8.0, 8.0, 2.0 Hz), 7.26 (dd, 1H, J = 7.6, 2.0 Hz), 6.71 (d, 1H, J = 8.8 Hz), 6.64 (ddd, 1H, J = 7.4, 7.4, 1.2 Hz). ^{13}C NMR (acetone-d_6): δ 173.9, 170.8, 167.6, 136.5, 136.2, 122.8, 119.2, 116.5, 58.9, 51.5, 34.1, 30.4, 26.8, 25.2, −6.9. LRMS (EI): M − CH$_3$+ = 332. HRMS (EI) M+ calcd for C$_{21}$H$_{36}$NO$_2$Ga: 332.0777. Found: 332.0778.

κ²*N*,*O*-4-(Phenyliminomethyl)benzene-1,3-diolatodimethylgallium (10a). ^{1}H NMR (acetone-d_6): δ 9.04 (s, 1H), 8.74 (s, 1H), 7.22 (t, 2H, J = 7.6, 7.6 Hz), 7.05 (m, 1H), 7.02 (d, 2H, J = 8.5 Hz), 6.86 (dd, 2H, J = 8.4, 1.2 Hz), 6.74 (d, 1H, J = 9.0 Hz), 6.73 (d, 2H, J = 8.5 Hz), 6.27 (d, 1H, J = 2.4 Hz), 6.10 (dd, 1H, J = 8.9, 2.4 Hz). ^{13}C NMR (acetone-d_6): δ 169.4, 169.0, 165.4, 137.9, 113.0, 107.0, 106.7, −6.9. LRMS (EI): M − CH$_3$+ = 388. HRMS (FAB) M+ Calcd for C$_{21}$H$_{20}$NO$_3$Ga: 404.0777. Found: 404.0777.

κ²*N*,*O*-4-[(4-Methoxyphenyl)phenyliminomethyl]benzene-1,3-diolatodimethylgallium (10b). ^{1}H NMR (acetone-d_6): δ 9.07 (s, 1H), 7.22 (dd, 2H, J = 7.6, 7.6 Hz), 7.11 (d, 2H, J = 8.8 Hz), 7.05 (t, 1H, J = 7.6 Hz), 6.89 (d, 2H, J = 7.3 Hz), 6.82 (d, 2H, J = 8.8 Hz), 6.28 (d, 1H, J = 2.4 Hz), 6.09 (dd, 1H, J = 8.9, 2.7 Hz), 3.75 (s, 3H), −0.48 (s, 6H). ^{13}C NMR (acetone-d_6): δ 176.0, 170.4, 164.3, 159.9, 145.9, 137.1, 131.1, 128.7, 125.3, 124.2, 112.9, 106.8, 105.6, 54.5, −8.8. LRMS (EI): M − CH$_3$+ = 402. Anal. Calcd for C$_{22}$H$_{22}$NO$_3$Ga: C, 63.19; H, 5.30; N, 3.35. Found: C, 63.13; H, 5.44; N, 3.18.

κ²*N*,*O*-2-(*tert*-Butyliminomethyl)-4-nitrophenolatodimethylgallium (11a). ^{1}H NMR (acetone-d_6): δ 8.81 (s, 1H), 8.48 (d, 1H, J = 2.9 Hz), 8.18 (dd, 1H, J = 9.3, 3.1 Hz), 6.80 (d, 1H, J = 9.3 Hz), 1.54 (s, 9H), −0.22 (s, 6H). ^{13}C NMR (acetone-d_6): δ 167.4, 136.5, 133.7, 130.2, 122.1, 117.7, 61.3, 29.3, −3.7. LRMS (EI): M − CH$_3$+ = 305. HRMS (FAB) M − CH$_3$+ Calcd for C$_{13}$H$_{19}$N$_2$O$_3$Ga: 305.0413. Found: 305.0417.

κ²*N*,*O*-1-Phenyl-2-(2-pyridyl)-1-ethenolatodimethylgallium (12a): Yellow solid. ^{1}H NMR (CDCl$_3$, 500 MHz): δ 7.86 (m, 3H), 7.63 (ddd, 1H, J = 8.3, 7.3, 1.7 Hz), 7.38 (m, 3H), 7.04 (dt, 1H, 7.0, 0.98 Hz), 6.99, (ddd, 1H, 7.3, 5.7, 1.3 Hz), 5.93 (s, 1H), −0.19 (s, 6H). ^{13}C NMR (CDCl$_3$, 125 MHz): δ 169.2, 156.9, 143.2, 140.1, 139.0, 129.3, 128.1, 126.4, 123.3, 118.3, 93.9, −7.65. MS (EI, 70 eV): m/z (relative intensity) 297 (M+, 5), 295 (M+, 8), 282 (68), 280 (100), 266 (8), 264 (12), 163 (8), 161 (11), 71 (90), 69 (14). Anal. Calcd for C$_{15}$H$_{16}$-GaNO: C, 60.86; H, 5.45; N, 4.73. Found: C, 60.84; H, 5.31; N, 4.76.

κ²*N*,*O*-1-(4-Hydroxyphenyl)-2-(2-pyridyl)-1-ethenolatodimethylgallium (12b): Yellow solid. ^{1}H NMR (CDCl$_3$, 500 MHz): δ 8.89 (bs, 1H), 7.70 (dd, 1H, J = 5.61, 1.65 Hz), 7.59 (AA′ of AA′XX′, 2H, J_{AX} = 8.60 Hz, J_{AA} = 2.48 Hz), 7.47 (ddd, 1H, J = 8.46, 7.06, 1.85 Hz), 6.89 (dt, 1H, J = 8.35, 1.04 Hz), 6.82 (ddd, 1H, J = 7.09, 5.76, 1.27 Hz), 6.724 (XX′ of AA′XX′, 2H, J_{AX} = 8.58 Hz, J_{XX} = 2.47 Hz), 5.73 (s, 1H), −0.35 (s, 6H). ^{13}C NMR (CDCl$_3$, 125 MHz): δ 168.9, 158.5, 156.7, 142.7,

138.5, 130.9, 127.7, 122.8, 117.4, 114.8, 92.0, −7.95. MS (EI, 70 eV): m/z (relative intensity) 313 (M+, 7), 311 (M+, 9), 298 (68), 296 (100), 282 (7), 280 (11), 179 (15), 177 (24), 149 (10), 148 (14), 121 (20), 71 (42), 69 (65). Anal. Calcd for C$_{15}$H$_{16}$-GaNO$_2$·0.5H$_2$O: C, 56.12; H, 5.34; N, 4.36. Found: C, 56.56; H, 5.32; N, 5.32.

κ²*N*,*O*-2-(5-Hydroxy-2-pyridyl)-1-phenyl-1-ethenolatodimethylgallium (12c): Yellow solid. ^{1}H NMR ((CD$_3$)$_2$CO, 500 MHz): δ 9.08 (bs, 1H), 7.86 (dd, 2H, J = 8.14, 1.57 Hz), 7.72 (d, 1H, J = 2.80 Hz), 7.48 (dd, 1H, J = 8.88, 2.77 Hz), 7.34 (m, 3H), 7.29 (d, 1H, J = 8.96 Hz), 6.11 (s, 1H), −0.29 (s, 6H). ^{13}C NMR (CDCl$_3$, 125 MHz): δ 165.6, 151.6, 150.7, 141.2, 130.8, 129.7, 129.4, 128.7, 126.7, 125.7, 93.6, −7.80. MS (EI, 70 eV): m/z (relative intensity) 313 (M+, 5), 311 (M+, 6), 298 (60), 296 (88), 282 (10), 280 (121), 212 (4), 184 (10), 163 (13), 161 (18), 149 (4), 148 (5), 105 (31), 77 (34), 71 (65), 69 (100). Anal. Calcd for C$_{15}$H$_{16}$GaNO$_2$: C, 57.74; H, 5.17; N, 4.49. Found: C, 57.59; H, 4.94; N, 4.27.

κ²*N*,*S*-1-Phenyl-2-(2-pyridyl)-1-ethene-1-thiolatodimethylgallium (12d): Yellow solid. ^{1}H NMR ((CD$_3$)$_2$CO, 500 MHz): δ 8.46 (dd, 1H, J = 5.47, 1.87 Hz), 8.10 (ddd, 1H, J = 8.15, 7.55, 1.76 Hz), 7.80 (m, 2H), 7.67 (ddd, 1H, J = 8.06, 1.30, 0.83 Hz), 7.55 (ddd, 1H, J = 7.42, 5.73, 1.33 Hz), 7.37 (m, 3H), 7.15 (s, 1H), −0.18 (s, 6H); ^{13}C NMR (CDCl$_3$, 125 MHz) ((CD$_3$)$_2$CO, 125 MHz): δ 155.6, 155.4, 146.4, 145.6, 141.5, 129.4, 128.8, 128.2, 128.1, 123.7, 121.2, −6.81. MS (EI, 70 eV): m/z (relative intensity) 313 (M+, 2), 313 (M+, 2), 298 (73), 296 (100), 212 (86), 180 (36), 152 (12), 78 (26), 71 (17), 69 (27). Anal. Calcd for C$_{15}$H$_{16}$GaNS: C, 57.73; H, 5.17; N, 4.49; S, 10.27. Found: C, 57.65; H, 5.18; N, 4.55; S, 10.04.

X-ray Structure Determination of 7c. Single crystals of **7c**, grown from a saturated CHCl$_3$ solution, were mounted on glass fibers with Paratone-N oil (Exxon) and immediately cooled to −75 °C in a cold nitrogen gas stream on the diffractometer. Standard peak search and indexing procedures gave rough cell dimensions, and least-squares refinement using 10 688 reflections yielded the cell dimensions given in Table 2. Data were collected with an area detector by using the measurement parameters listed in Table 2. Systematic absences for 0*kl* ($k + l \neq 2n$) and *hk*0 ($h \neq 2n$) were consistent with space groups *Pnma* and *Pna*2$_1$. The average values of the structure factors suggest the centri choice *Pnma*, which was verified by the successful refinement of the structure. The measured intensities were reduced to structure factor amplitudes and their esd's by correction for background and Lorentz and polarization effects. While corrections for crystal decay were unnecessary, a face-indexed absorption correction was applied, the maximum and minimum transmission factors being 0.858 48 and 0.570 50. Systematically absent reflections were deleted and symmetry equivalent reflections were averaged to yield the set of unique data. All 10 688 data were used in the least-squares refinement. The structure was solved using direct methods (SHELXTL). The correct positions for the C, O, and Ga atoms were deduced from an E-map. Subsequent least-squares refinement and difference Fourier calculations revealed the positions of the remaining non-hydrogen atoms. The quantity minimized by the least-squares program was $\sum w(F_o^2 - F_c^2)^2$, where $w = [[\sigma(F_o^2)]^2 + (0.0765P)^2 + 3.6495P]^{-1}$ and $P = (F_o^2 + 2F_c^2)/3$. The analytical approximations to the scattering factors were used, and all structure factors were corrected for both real and imaginary components of anomalous dispersion. In the final cycle of least squares, independent anisotropic displacement factors were refined for the non-hydrogen atoms and the aromatic, vinyl, and methyl hydrogen atoms were fixed in "idealized" positions, with C−H = 0.95 Å for the aromatic and vinyl hydrogens and C−H = 0.98 Å for the methyl hydrogens. Successful convergence was indicated by the maximum shift/error of 0.001 for the last cycle. Final refinement parameters are given in Table 2. The largest peak in the final Fourier difference map (1.966 e Å^{-3}) was located 0.88 Å from C10. A final analysis of

variance between observed and calculated structure factors showed no apparent errors.

X-ray Structure Determination of 12a. Single crystals of **12a** were grown and mounted the same as described for compound **7a** above. Standard peak search and indexing procedures gave rough cell dimensions, and least-squares refinement using 8701 reflections yielded the cell dimensions given in Table 2. Data were collected with an area detector by using the measurement parameters listed in Table 2. Systematic absences for $0k0$ ($k \neq 2n$) and $h0l$ ($h + l \neq 2n$) were consistent only with space group $P2_1/n$. The measured intensities were reduced to structure factor amplitudes and their esd's by correction for background and Lorentz and polarization effects. While corrections for crystal decay were unnecessary, a ψ-scan absorption correction was applied, the maximum and minimum transmission factors being 0.990 and 0.861. Systematically absent reflections were deleted and symmetry equivalent reflections were averaged to yield the set of unique data. All 8701 data were used in the least-squares refinement. The structure was solved using direct methods (SHELXTL). The correct positions for the C, N, O, and Ga atoms were deduced from an E-map. Subsequent least-squares refinement and difference Fourier calculations revealed the positions of the remaining non-hydrogen atoms. The quantity minimized by the least-squares program was $\sum w(F_o^2 - F_c^2)^2$, where $w = [[\sigma(F_o^2)]^2 + (0.0138P)^2 + 1.3221P]^{-1}$ and $P = (F_o^2 + 2F_c^2)/3$. The analytical approximations to the scattering factors were used, and all structure factors were corrected for both real and imaginary components of anomalous dispersion. In the final cycle of least squares, independent anisotropic displacement factors were refined for the non-hydrogen atoms, and the aromatic, vinyl, and methyl hydrogen atoms were fixed in "idealized" positions, with C$-$H = 0.95 Å for the aromatic and vinyl hydrogens and C$-$H = 0.98 Å for the methyl hydrogens. Successful convergence was indicated by the maximum shift/error of 0.001 for the last cycle. Final refinement parameters are given in Table 2. The largest peak in the final Fourier difference map (0.330 e Å^{-3}) was located 0.88 Å from C14. A final analysis of variance between observed and calculated structure factors showed no apparent errors.

Hydrolysis Studies. A weighed sample of each gallium complex was dissolved in acetone-d_6 to form a 0.20 M solution. At room temperature, H_2O was added to achieve a H_2O/Ga ratio of 1000. Formation of $(CH_3)_2GaOH$ was monitored by ^{1}H NMR, with the percent hydrolysis measured by integrating the $(CH_3)_2Ga-$ peaks corresponding to the unhydrolyzed complex and to $(CH_3)_2GaOH$. The determination of percent hydrolysis was made 12$-$24 h after the addition of H_2O. These percent hydrolysis values are listed in Figure 2.

Supporting Information Available: Full crystallographic information, atomic coordinates and isotropic displacement parameters, and intramolecular bond distances and angles can be found on pages S-2$-$10 for compound 7c and pages S-11$-$17 for compound **12a**; experimental procedures and characterization for all ligands can be found on pages S-18$-$27 (28 pages). Ordering information can be found on any current masthead page.

OM980413X